Nat. Volatiles & Essent. Oils, 2021; 8(4): 3849-3878

NVEO
Natural Volatiles &
Essential Oils

Gene Expressions Of C9ORF72 And Rab7A During Endoplasmic Reticulum (ER) Stress In Familial Amyotrophic Lateral Sclerosis (FALS)

Intan Barul Akma Bakhtiar[a,b*] and Jacqueline deBelleroche[a]

[a] Neurogenetics Group, Department of Brain Sciences, Faculty of Medicine, Imperial College London, London, UK.

[b]Faculty of Allied Health Sciences, University of Cyberjaya, Persiaran Bestari 1, Cyber 11, 63000 Cyberjaya, Selangor, Malaysia.

Email intan.akma@cyberjaya.edu.my

ABSTRACT

The non-coding hexanucleotide repeat expansions (HRE) in intron 1 of theC9ORF72gene have been identified as the most frequent genetic cause of familial ALS and familial frontotemporal degeneration (FTD).In this report, we studied the effect of C9ORF72 HREduring ER stress in lymphoblastoid cell lines (LCLs) derived from familial ALS and healthy controls and explore the C9ORF72role in the pathogenesis of ALS. In order to investigate the pathogenic effects of this mutation, the gene expression approach was applied through cell culture, quantitative PCR, RNA and protein extractions and Western blotting.Here, we showed that C9ORF72 isoform a and bmRNA expressions were upregulated in the C9-positive lymphoblastoid cell lines in basal condition. We also showed that Rab7a mRNA level was also upregulated in the C9-positive FALS cell lines compared to wild types in basal condition. During ER stress, C9ORF72 isoform a mRNA level was downregulated whereas C9ORF72 isoform b and Rab7a mRNA levels were upregulated. Western blotting analysis of C9ORF72-L protein showed a downregulation trend in the C9-positive cell lines during ER stress. Our study therefore further provides a strong evidence of autophagy involvement in C9ORF72-ALS. Therefore, the study indicated that endoplasmic reticulum (ER) stress might aggravate C9ORF72 HRE effect in FALS lymphoblastoid cell lines particularly in autophagyas an important pathway in C9 ALS/FTD pathogenesis.Our data indicated that the percentage of apoptotic cells was higher in C9-positive cell lines with or without staurosporine treatment when comparing to wild types, therefore suggesting C9 HRE may aggravate cell death in lymphoblastoid cell lines. The upregulation of lymphoblastoid cells apoptosis may be achieved by the activation of pro-apoptotic pathways or inactivation of anti-apoptotic pathways

Keywords: Amyotrophic lateral sclerosis, C9ORF72, Rab7A, autophagy, ER stress, apoptosis.

INTRODUCTION

Amyotrophic lateral sclerosis (ALS) is a fatal neurodegenerative disease that is characterised by the loss of upper motor neurons in motor cortex and lower motor neurons in the brainstem and spinal cord, that results in progressive paralysis and death due to respiratory failure (1). Familial ALS (FALS) accounts for approximately ~5 to 10% of ALS cases whilst the rest of ALS cases are sporadic (2). The C9ORF72 geneis located on chromosome 9p21.2and the gene gives rise to three transcripts which are variant 1(V1, NM_145005.6), variant 2 (V2, NM_0.18325.4) and variant 3 (V3, NM_001256054.2). Variant 2 and variant 3 encode for C9ORF72 isoform a (long isoform; C9ORF72-L) that consists of 481 amino acids, whereas variant 1 encodes for C9ORF72 isoform b (short isoform; C9ORF72-S) that comprises of 222 amino acids (Figure 1). Genetic linkage analysis of a Scandinavian family with multiple family members affected with ALS and FTD had originally identified a locus on chromosome 9p21.3-p13.3 to be linked to ALS-FTD (3). Since then, hexanucleotide repeat expansions (HRE) in C9ORF72 have been identified as the most frequent genetic cause of familial ALS and familial frontotemporal degeneration (FTD) (4, 5).The number of HREs in the intronic region of C9ORF72 varies from thirty to several hundred repeats (6). C9ORF72 HREs give rise to a more aggressive form of ALS than other mutation, where patients with HRE have an earlier age at onset, about ~2.5 years earlier than patients without the repeat expansions and are more likely to have a positive family history of dementia (6). ALS patients carrying C9ORF72 HREs are indistinguishable from classic ALS patients but nearly 50% of the C9-positive ALS cases develop cognitive or behavioural impairment or both, compared to those without HRE where these features are less common (7, 8). C9ORF72 protein is structurally homologous to Differentially Expressed in Normal and Neoplasia (DENN) proteins that act as Guanine nucleotide exchange factors (GEFs) to activate RAB GTPases and may therefore, regulate membrane trafficking (9, 10).

The endoplasmic reticulum (ER) is responsible for protein synthesis, folding and maturation of secretory and transmembrane proteins and lipid biosynthesis(11).ER stress occurs when there are accumulations of misfolded or unfolded proteins in the organelle (11, 12). In chronic or irreversible ER stress in which the cells cannot mitigate the ER stress, the unfolded protein response (UPR) results in apoptotic cell deaths (13, 14). Apoptosis is a programmed cell death that is identified by cell shrinkage, cell surface blebbing, organelle contraction, apoptotic bodies formation, chromatin condensation and nuclear fragmentation (15). As ALS is characterised by the loss of motor neurons, it is suggested that apoptosis is the cause of motor neuron cell death (15). Apoptosis is detected in the brain and spinal cord of SALS individuals by TUNEL staining (16). Cell apoptosis is also increased in SOD1 mutant mice (17, 18).

Here, we examined the effect of C9ORF72 HREon ER stress and apoptosis and its association with ALS and proposed consequences on cellular pathways.

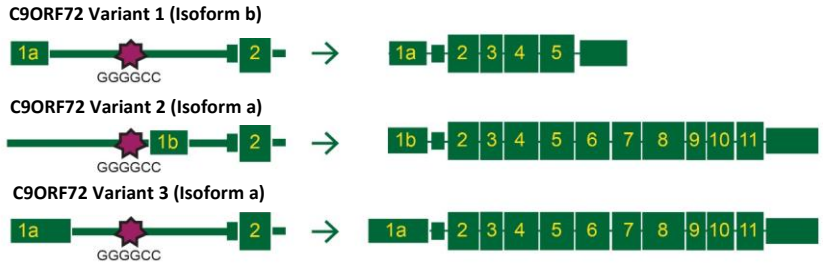

Figure 1: The C9ORF72 hexanucleotide repeat expansions. This schematic diagram shows the sites of C9ORF72 hexanucleotide repeat expansions, GGGGCC depicted as stars and the three annotated transcript variants; variant 1, variant 2 and variant 3. The pathogenic C9ORF72 HRE is found in the first intron of the variant 1 and variant 3 and is located within the predicted promoter region of variant 2.(Image: Own work).

MATERIALS AND METHODS

Cell culture

Lymphoblastoid cell lines (LCLs) from 12 families harbouring C9ORF72 hexanucleotide repeat expansions (HRE) were cultured at 37˚C and 5% CO_2 in RPMI-1640 medium (Gibco) containing 10% foetal bovine serum (FBS) (Sigma-Aldrich), 1% Penicillin/Streptomycin (Gibco) and 1% glutamax (Gibco).

Extraction of mRNA and cDNA Synthesis

In brief, mRNA was extracted from tissues with the Direct-Zol RNA MiniPrep(Zymo Research) and reverse transcribed to cDNA using approximately 1ug of RNA with random hexamers 50uM (Invitrogen, US), AMV Reverse Transcriptase (New England Biolab), 40mM dNTP Mix (Bioline) and DEPC-treated water (Invitrogen), following which cDNA samples were stored at -20°C until further use. RNA purity and integrity for all sampleswas assessed by using multiple well-established methods.

Quantitative Polymerase Chain Reaction (qPCR)

Primers were designed using Primer 3 web software to amplify the target cDNA sequence and are listed in the Table S1 in Supplementary Materials. Quantitative PCR (qPCR) was performed using the Power Up™ SYBR™ Green Master Mix (ThermoFisher Scientific) and amplification was carried out using an Mx3000P Real-time PCR System (Stratagene).The following cycling conditions were applied:

initial denaturation at 95°C for 10 min followed by 35 cycles each with denaturation at 95°C for 30 sec, annealing at an optimised temperature for 30 sec and extension at 72°C for 45 sec. A final cycle of denaturation at 95°C for 1 minute, annealing at an optimised temperature for 30 sec and extension at 95°C for 45 sec was also included. All the amplified qPCR products were analysed by observing thermal dissociation curves and using gel electrophoresis to ensure the purity and sizing of the single product. The samples were normalised against the housekeeping gene, GAPDH.

Protein extraction

The proteins were extracted from LCLs with RIPA buffer containing a cocktail of protease inhibitors and phosphatase inhibitor. Protein extracts were then placed at 4˚C for 1 hour, centrifuged at 12 000 rpm for 20 minutes at 4˚C and the supernatant stored at -80˚C. Protein concentrations were determined using a Bio-Rad protein assay kit.

Western blotting

Denatured protein samples (25µg) were electrophoresed into polyacrylamide gel electrophoresis (SDS-PAGE) and electrophoresed with 1x FASTRun Tris SDS PAGE Running Buffer (Fisher Bioreagents) at 200V for about 1 hour. Spectra™ Multicolour Broad Range Protein Ladder (ThermoFisher Scientific) was used for protein size standards. Gels were transferred to nitrocellulose membranes(Amersham Hybond™ ECL™, GE Healthcare)then placed in blocking solution 5% skimmed milk powder(Sigma-Aldrich) and washed three times with PBS (Fisher Bioreagents) containing 0.01% Tween-20 (PBST) (Fisher Bioreagents). Incubated with the primary antibody(anti-C9ORF72 for overnight at 4˚C; anti-GAPDH for2 hours at 4˚C). After three times washes with PBST, incubated with the secondary antibody for 1 hour at room temperature. Antibody labelling was visualised using Pierce™ ECL western blotting substrate(ThermoFisher Scientific) and assayed on the machine. Band intensity was measured using ImageJ software (1.47v)(National Institutes of Health) and normalised with respect to the loading controls. Antibodies used wereanti-C9ORF72 (22637-1-AP) from ProteinTech and anti-GAPDH (0411): sc-47724 from Santa Cruz Biotechnology.

FITC annexin V assay

3 x 10^6 cells LCLs were seeded in a 24-well plate and incubated in 10% FBS/RPMI (Sigma-Aldrich). After 24 hours, cells were treated with 0.5 µM thapsigargin (Sigma-Aldrich) or 2 µg/ml tunicamycin (Sigma-Aldrich) for 6 hours.The drug treatment was inhibited with the addition of cold PBS (Fisher Scientific). After treatment, the cells were pelleted and stained using the FITC-Annexin V Apoptosis Detection Kit I (BD Biosciences) according to the manufacturer's protocol and were analysed by the flow cytometry.

Staurosporine treatment and cell survival assay

Cells were seeded at a density of 3 x 10^6 cells per well for approximately 24 hours before treatments were added. Experimental treatments of 3µM or 5 µM staurosporine (Sigma-Aldrich) were added to the cultured LCLs for a time course ranging from 2 to 24 hours. After treatments, the cells were pelleted and stained using the FITC-Annexin V Apoptosis Detection Kit I (BD Biosciences) according to the manufacturer's protocol. The cells were further analysed with a fluorescence-activated cell sorting (FACS) flow cytometer (BD Biosciences).

Statistical analysis

Statistical analysis was performed using GraphPad Prism software. The effect of the mutation was analysed using unpaired or paired Student's t-test (parametric) accordingly. The effect of the mutation together with drug treatment was analysed using two-way ANOVA with a Bonferroni post-hoc test. $p<0.05$ was considered to indicate a statistically significant result. Results were given as mean ± standard error of the mean (SEM).

RESULTS

Gene expressions of C9ORF72 isoform a and b in basal condition

We investigated the levels of C9ORF72 isoform a and b mRNAs in lymphoblastoid cell lines (LCLs) obtained from healthy controls and FALS patients in basal condition using quantitative PCR (qPCR). Previous works on LCLs have found that both C9ORF72 isoform a and b mRNA levels were reduced in C9 HRE carriers compared to healthy subjects (4, 19, 20). Contrarily, we observed significant upregulations in the C9ORF72 isoform a and isoform b mRNA levels in FALS patients carrying C9 HRE compared to healthy subjects (Figure 2). The previously mentioned studies however, have a limited number of samples and some of the studies used LCLs generated from ALS and FTD patients carrying C90RF72 HRE whereas our study has a bigger sample size and utilized LCLs from FALS patients carrying the C9ORF72HRE.

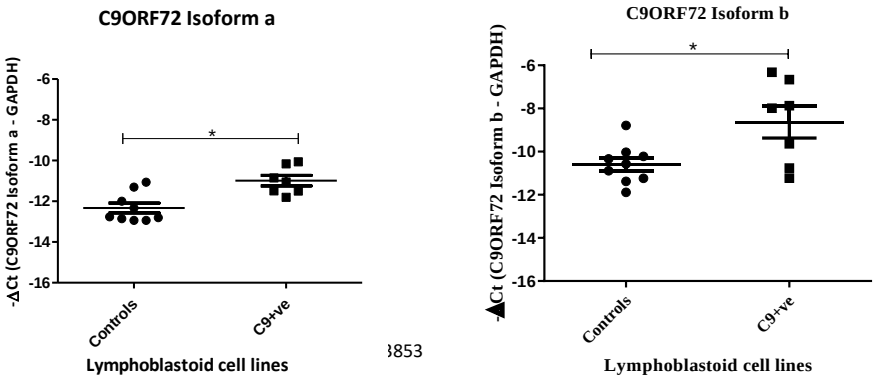

Figure 2:qPCR analysis of C9ORF72 isoform a and b mRNAs from lymphoblastoid cell lines normalised against GAPDH. Unpaired t tests were used to compare C9ORF72 isoforms expression between C9-positive (C9+ve) and control individuals.*,p<0.05

Gene expressions of C9ORF72 isoform a and b under ER stress conditions

We compared the C9ORF72 isoform a and b expressions in wild type and C9-positive FALS under ER stress (Figure 3). In this study, we employed tunicamycin and thapsigargin to elicit the ER stress response in lymphoblastoid cell lines. Tunicamycin inhibits the initial step of glycoprotein biosynthesis resulting in the accumulation of unfolded glycoproteins in the ER therefore, causing ER stress (21).Thapsigargin is a specific inhibitor of the sarcoplasmic/endoplasmic reticulum Ca^{2+}-ATPase (SERCA) that decreases calcium levels in ER resulting in calcium-dependent ER chaperones for example, calnexin to lose their chaperone activity (22).We observed that C9ORF72 isoform a mRNA level was significantly downregulated in C9-positive cell linescompared to wild typesin DMSO and following tunicamycin treatment. Interestingly, wild types displayed significant upregulations of isoform a following ER stress treatments compared to DMSO. Further, we found isoform b mRNA levels were significantly elevated in C9-positive subjects compared to wild types in DMSO and upon treatments with tunicamycin and thapsigargin. C9-positive cell lines also showed a significant upregulation of isoform b mRNA in thapsigargin compared to DMSO.

Commented [dBJS1]: This section should go into the introduction to Chapter 6 not after you have started describing the results

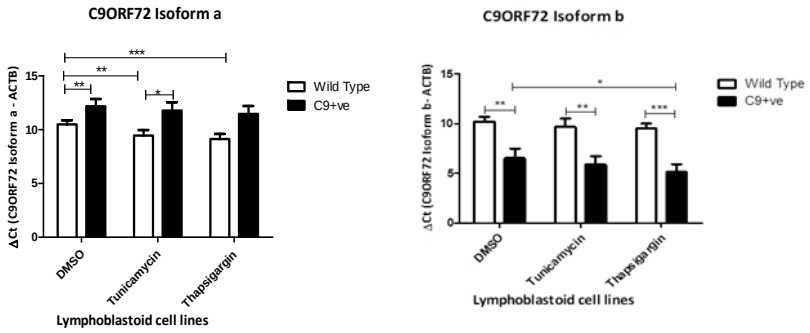

Figure 3: qPCR analysis of C9ORF72 isoform a and b mRNA levels from lymphoblastoid cell lines normalised against ACTB between C9-positive and controls, with and without ER stress.The data is given as ΔCt and is represented by means and SEMs.*,p<0.05,**,p<0.01, ***,p<0.001

The antibody was raised to residues 1-169 amino acids within the N-terminal region of C9ORF72 protein. A BLAST search using these specific sequences showed no homology with other proteins. We observed that lysates from lymphoblastoid cell lines show a distinct single protein band at

approximately 54 kDa (Figure 4) which corresponds to the predicted molecular weight of C9ORF72-L, that is 54.3 kDa. Western blot analysis showed there was no change in C9ORF72-L protein levels between wild types and C9-positive lymphoblastoid cell lines in DMSO or following treatment with tunicamycin or thapsigargin.

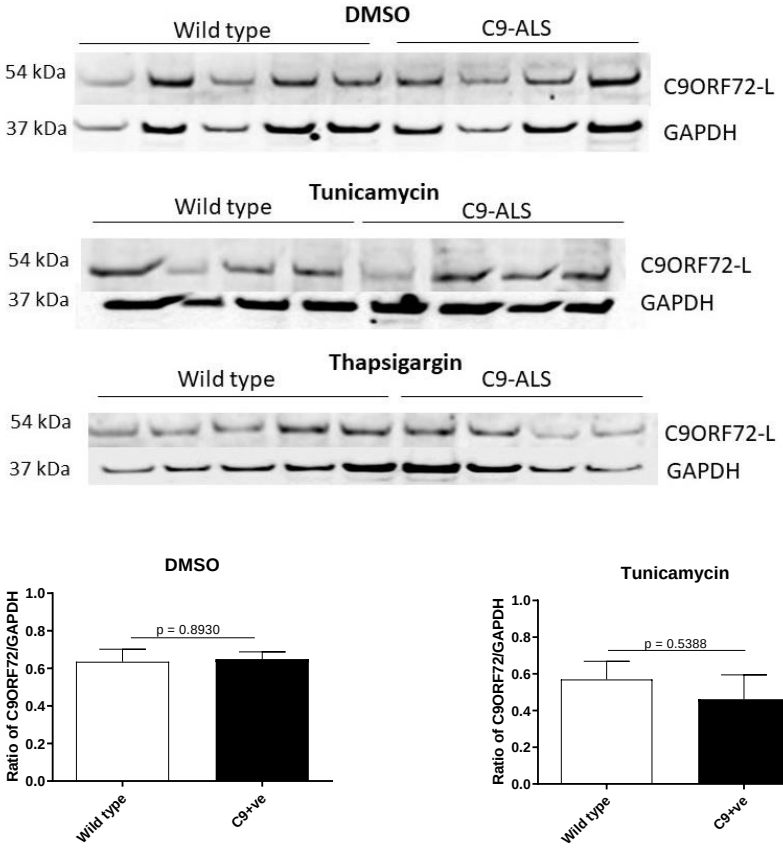

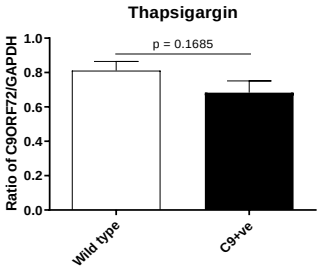

Figure 4: C9ORF72-L protein expressions. The LCLs were treated with tunicamycin and thapsigargin and the C9ORF72-L protein levels were investigated at basal level and under cellular stress condition. There was no change in C9ORF72-L protein levels observed between wild types and C9-positive lymphoblastoid cell lines in DMSO or following tunicamycin and thapsigargin treatment.

Gene expression of Rab7 in basal condition and under ER stress

Rab7 mRNA level was significantly increased in C9 HRE carriers compared with healthy controls in basal condition (Figure 5).In wild types,there were significant upregulations in Rab7 mRNA level in ER stress treatments compared to no treatment. As shown in Figure 6, there was a non-significant upregulation of Rab7 mRNA level in C9-positive cell lines when treated with thapsigargin compared to no treatment (p = 0.0718).No difference was observed between wild type and C9-positive cell lines in basal condition and under ER stress.

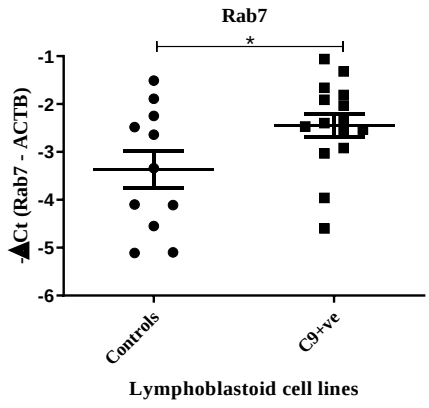

Figure 5: Quantitative PCR analysis of Rab7 mRNA in the lymphoblastoid cell lines normalised against ACTB showed the Rab7 expression was increased in FALS C9-positive compared with control individuals. *,p <0.05

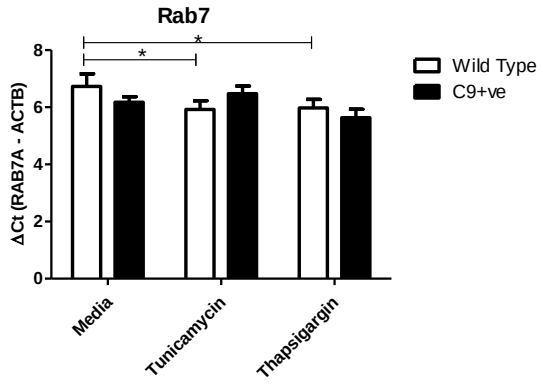

Figure 6: qPCR analysis of Rab7 mRNA level from lymphoblastoid cell lines normalised against ACTB between C9-positive and controls, with and without ER stress.*,p <0.05

Effect of the mutation on the expression of ER stress responsive genes

Given that tunicamycin and thapsigargin can activate ER stress and that excess ER stress leads to apoptosis, we determined the expressions of ER stress-associated genes (XBP1s, DNAJB9 (ERdj4) and HSPA5) in the cell lines.The results also showed that XBP1s and DNAJB9 were upregulated in wild types and C9-positive cell lines whereas HSPA5 mRNA levels showed a significant decrease in C9 HRE carriers compared to wild types upon tunicamycin treatment. This might indicate that HSPA5 function is impaired in C9-positive cell lines therefore, affecting the UPR signalling network and causing ER stress leading to the pathogenesis of ALS.

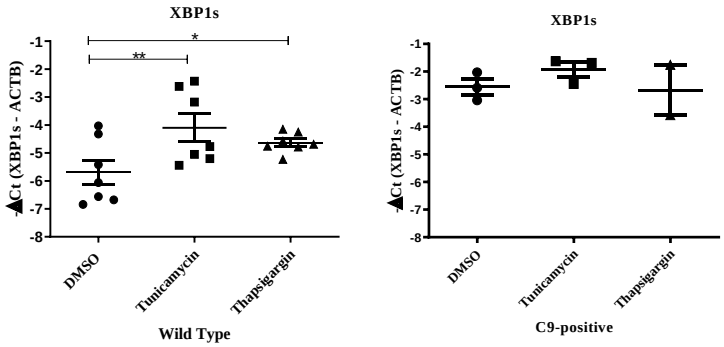

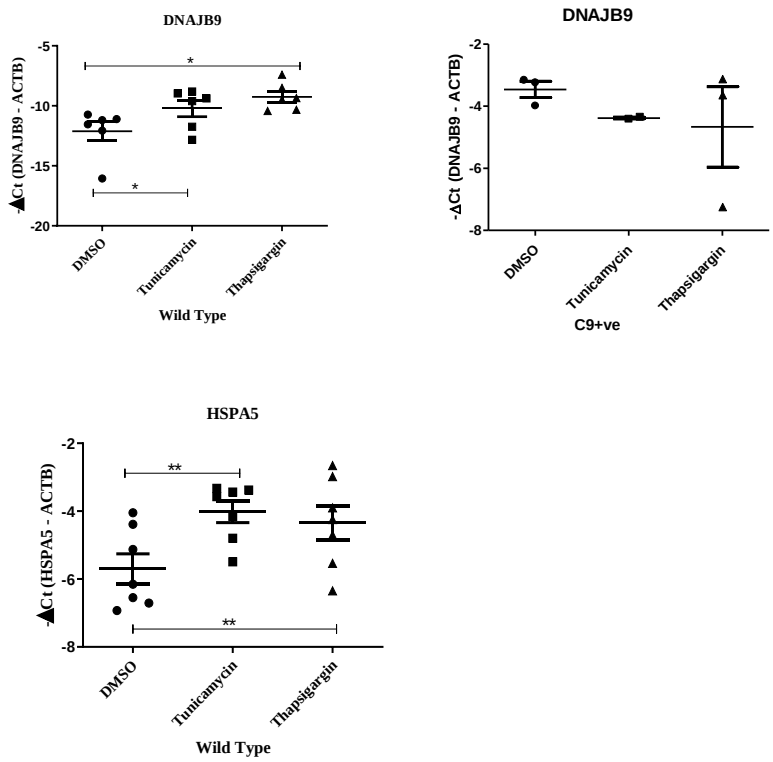

Figure 7: Relative changes in XBP1s, DNAJB9 (ERdj4) and HSPA5 mRNA levels in DMSO, thapsigargin and tunicamycin treated cells relative to the ACTB mRNA level. In wild types, there was a significant upregulation of XBP1s, DNAJB9 and HSPA5 mRNA levels following tunicamycin and thapsigargin treatment whilst there was no difference in C9-positive cell lines.*,p <0.05,**,p<0.01

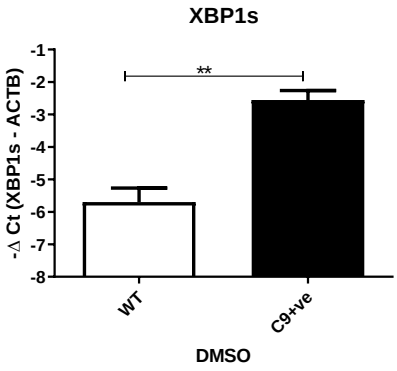
XBP1s
-Δ Ct (XBP1s - ACTB)
-1
-2
-3
-4
-5
-6
-7
-8
**
WT
C9+ve
DMSO

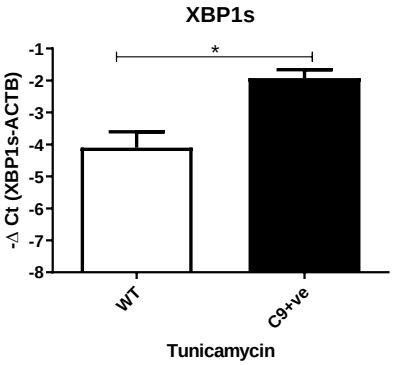
XBP1s
-Δ Ct (XBP1s-ACTB)
-1
-2
-3
-4
-5
-6
-7
-8
*
WT
C9+ve
Tunicamycin

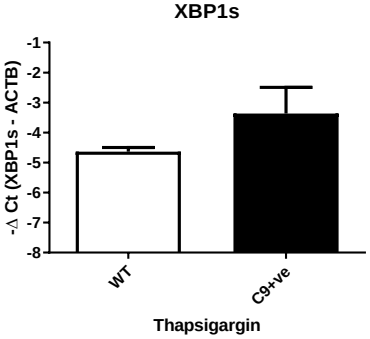
XBP1s
-Δ Ct (XBP1s - ACTB)
-1
-2
-3
-4
-5
-6
-7
-8
WT
C9+ve
Thapsigargin

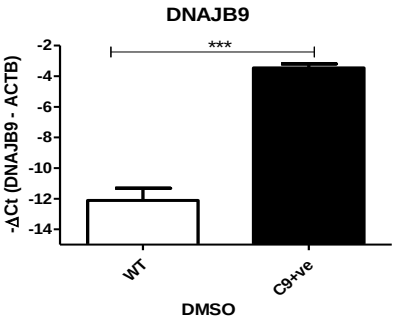
DNAJB9
-ΔCt (DNAJB9 - ACTB)
-2
-4
-6
-8
-10
-12
-14
***
WT
C9+ve
DMSO

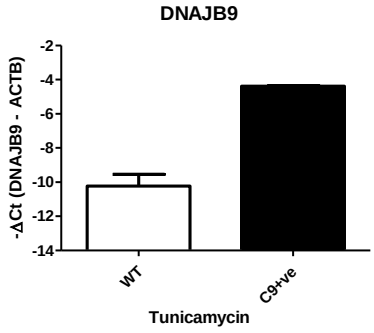
DNAJB9
-ΔCt (DNAJB9 - ACTB)
-2
-4
-6
-8
-10
-12
-14
WT
C9+ve
Tunicamycin

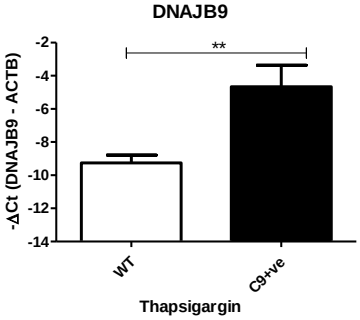
DNAJB9
-ΔCt (DNAJB9 - ACTB)
-2
-4
-6
-8
-10
-12
-14
**
WT
C9+ve
Thapsigargin

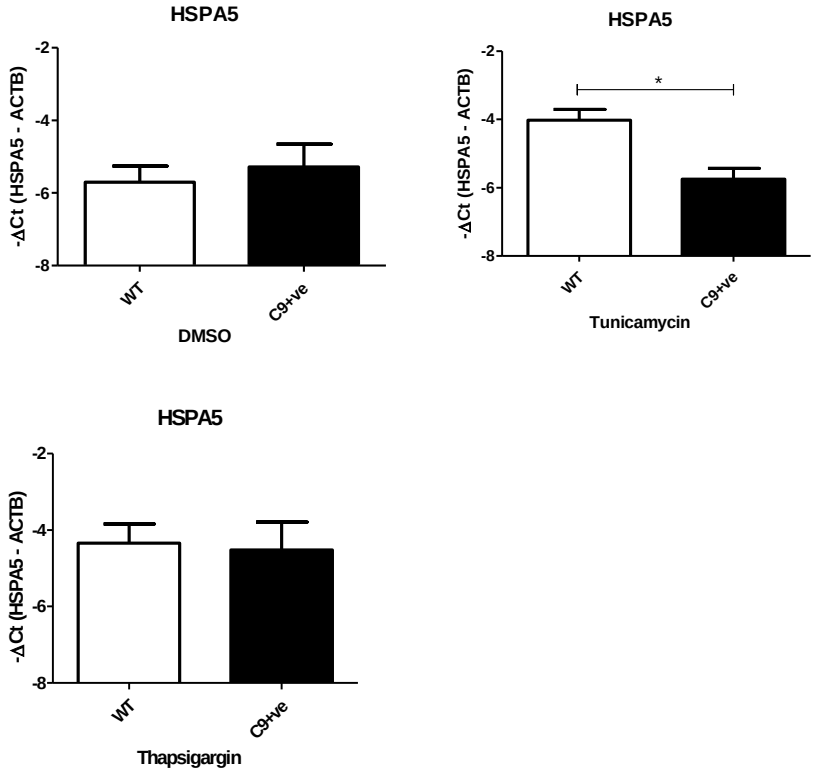

Figure 8: The mRNA levels of the ER stress genes (XBP1s, DNAJB9 and HSPA5) that were affected by the mutation at basal levels and under cellular stress in wild-types and C9-positive cell lines. The C9ORF72 HRE significantly decreased the expression of the marker gene of the ER stress pathway, HSPA5. The gene expression levels were normalised to ACTB.*,p <0.05, **,p<0.01,***,p<0.001

Effect of the C9ORF72 Hexanucleotide Repeat Expansions (HRE) in ER stress in the Lymphoblastoid Cell Lines

As shown in Figure 9, tunicamycin and thapsigargin were able to induce significant upregulations in the total apoptosis in wild types and C9-positive cell lines. Following tunicamycin treatment, there was also a non-significant upregulation in the total apoptosis events in C9-positive cell lines as compared to wild types (p = 0.0860) whereas the percentages of total apoptosis events in wild types and C9-positive cell lines were almost similar following thapsigargin treatment. In wild types, the percentage of total apoptosis events was significantly higher following thapsigargin treatment than tunicamycin whereas there was no difference in the total apoptosis events between tunicamycin and thapsigargin exposures in C9-positive cell lines.

There was no difference in necrosis in wild types with or without ER stress treatments. In C9-positive cell lines, there were upregulations of necrotic cells following ER stress treatments. There was no difference in necrosis between wild types and C9-positive cell lines with or without tunicamycin and thapsigargin exposures.

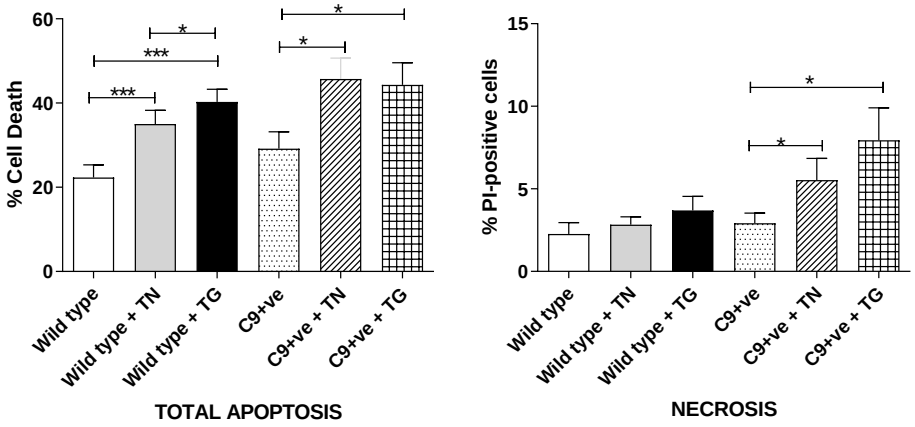

Figure 9: The rates of (A) total apoptosis and (B) necrosis in wild types (n = 12) and C9ORF72-positive cell lines (n = 12) upon treatment with 2 µg/ml tunicamycin (TN) and 0.5 µM thapsigargin (TG)for 6 hours. (A) Tunicamycin and thapsigargin were able to induce significant upregulations in the total apoptosis in both wild types and C9ORF72-positive cell lines. There was no significant difference in the percentage of total apoptosis between wild types and C9ORF72-positive cell lines. (B) Tunicamycin and thapsigargin induced significant increases of necrotic cells in C9ORF72-positive cell lines. *,p<0.05, **,p<0.01,***,p<0.001

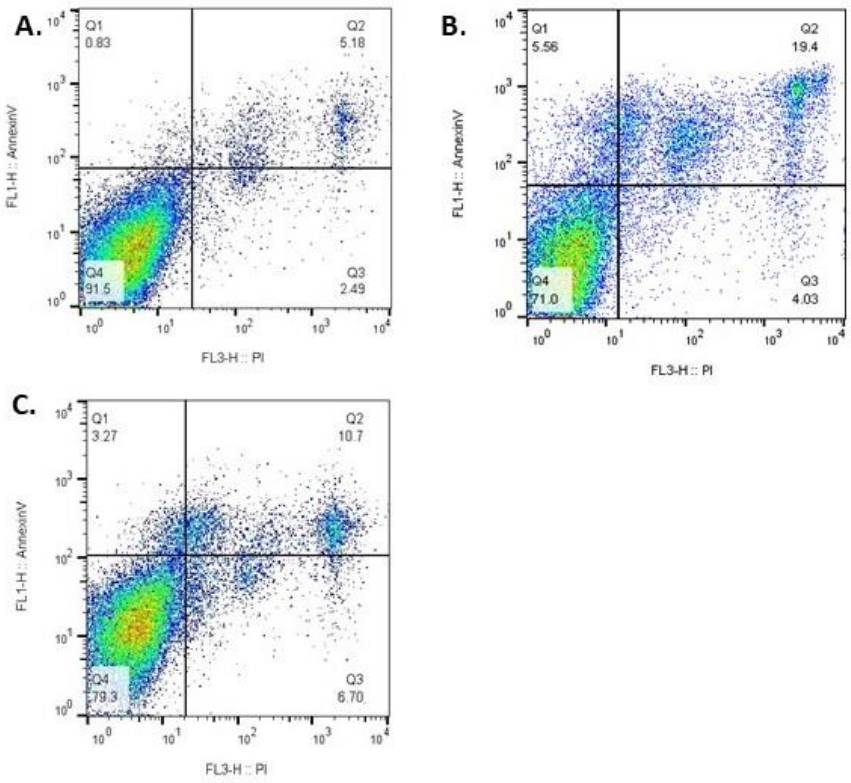

Figure 10: Representative of a wild type cell line from the C9-ALS families treated with tunicamycin and thapsigargin. Dot blot graphs from flow cytometric analysis show the rate of apoptosis and necrosis in the wild type treated with tunicamycin or thapsigargin for 6 hours. The percentages of early, late apoptotic, necrotic and live cells are indicated. (A) Wild type without treatment, (B) Wild type with tunicamycin treatment, (C) Wild type with thapsigargin treatment, (Quadrant 1:Early apoptotic cells, Quadrant 2:Late apoptotic cells, Quadrant 3:Live cells and Quadrant 4:Necrotic cells).

Cell survival assay

Next, we examined the effect of staurosporine in lymphoblastoid celllines carrying the C9ORF72 HRE. We first measured apoptosis in lymphoblastoid cell lines exposed under different conditions of staurosporine treatment. The cells were exposed to 3 µM or 5 µM staurosporine in different incubation times; 2, 4 and 24 hours (Figure 11, Table S2). At staurosporine 3 µM, total apoptosis events were consistent for 0-4 hours for wild types (21-24%) and C9-positive cell lines (25-26%) and

were increased to more than half of the cells population, in both wild types and C9-positive cell lines after 24 hours.

When increasing the staurosporine treatment to 5 µM, total apoptosis were consistent (21-22%) for wild type cell lines in different incubation times for 0 hour, 2 hours,4 hours and 24 hours incubation. In the C9-positive cell line, total apoptosis were consistent (17-18%) in 0 and 2 hours treatment but were increased at 4 hours.

The concentration of 3 µM staurosporine for 24 hours resulted in more than half of cells population died whereas using staurosporine 5 µM for 24 hours resulted in the majority of the cells went into necrosis stage. Because our study was aimed at understanding the effects of C9 HRE on staurosporine-induced apoptosis in lymphoblastoid cell lines, these effects were not desirable therefore,staurosporine 5 µMexposure for 4 hours sufficiently induced apoptosis in LCLs.

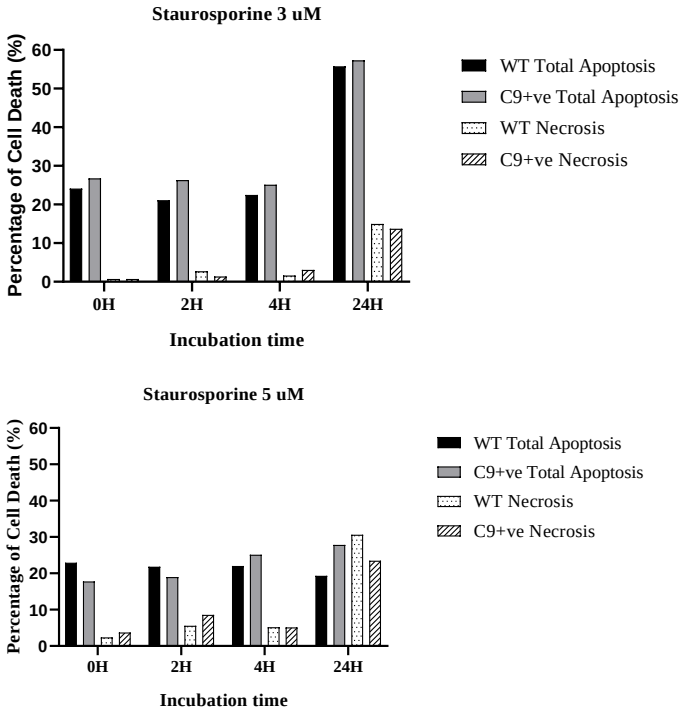

Figure 11: The rates of total apoptosis and necrosis in wild type (WT) and C9ORF72-positive (C9) cell lines upon treatment with 5 and 3 µM staurosporine for 0, 2, 4 and 24 hour(s).

Next, the effects of staurosporine at 5 µM for 4 hours treatment on apoptosis and necrosis events in the lymphoblastoid cell lines were investigated.Overall, staurosporine was able to elicit a significant increase in total apoptosis in the wild type and C9-positive cell lines upon treatment with staurosporine(Figure 12, Table S3). There was no difference in the total apoptosis rates between wild type and the C9-positive cell lines without staurosporine treatment. There was a non-significant increase in theC9-positive cell lines comparing with wild typesafter staurosporine treatment(p = 0.0833).Furthermore, necrosis was increased significantly in wild types and C9-positive cell lines after staurosporine treatment.These results indicated complete cell deaths in the wild type and C9-positive cell lines were achieved.

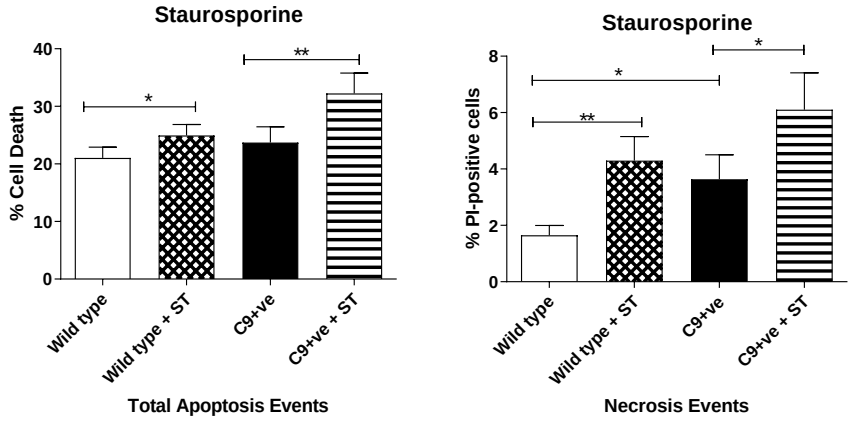

Figure 12: The rates of total apoptosis and necrosis in wild types (WT) and C9ORF72-positive (C9) cell lines were increased significantly upon treatment with 5 µM staurosporine (ST) for 4 hours.Without staurosporine treatment, there was a significant increase of the necrosis rates in the C9-positive cell lines compared to wild types.*,p <0.05, **,p<0.01

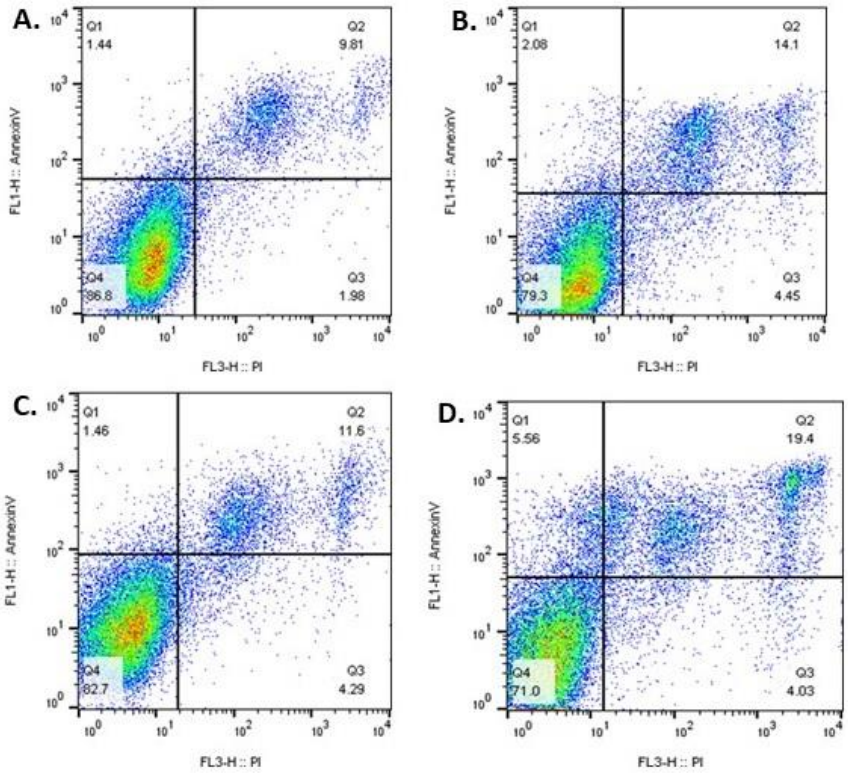

Figure 13: Representatives of lymphoblastoid cell lines treated with staurosporine. Dot blot graphs from flow cytometric analysis show the rate of apoptosis and necrosis in wild type and C9-positive cell lines treated with staurosporine at 5 µM for 4 hours. The percentages of early, late apoptotic, necrotic and live cells are indicated. (A) Wild type at 0 hour, (B) Wild type after 4 hours treatment, (C) C9ORF72-positive at 0 hour and (D) C9ORF72-positive after 4 hours treatment. (Quadrant 1:Early apoptotic cells, Quadrant 2:Late apoptotic cells, Quadrant 3:Live cells and Quadrant 4:Necrotic cells).

DISCUSSION

C9ORF72 uses alternative splicing to produce three different transcript variants in which Variant 2 and Variant 3 encode a long isoform (isoform a), whereas Variant 1 encodes a short isoform (isoform b). Bioinformatics studies showed that C9ORF72 may contain Differentially Expressed in Normal and Neoplastic cells (DENN) domain that is known to be involved in Rab-dependent intracellular trafficking (9, 23). The lymphoblastoid cell lines (LCLs) from ALS patients harbouring hexanucleotide repeat expansions (HRE) in C9ORF72 is a robust model to study the effect of C9ORF72 mutation on neuronal death in ALS which would otherwise be challenging to obtain due to the large size of the pathological repeats. Previous works on LCLs have found that both C9ORF72 isoform a and b mRNA levels were reduced in C9 HRE carriers compared to healthy subjects (4, 19, 20).Contrary to expectation, we observed significant upregulations in the C9ORF72 isoform a and isoform b mRNA levels in FALS patients carrying C9 HRE compared to healthy subjects that suggest the C9ORF72 isoform a and b are upregulated in the diseased state therefore forming toxic RNA foci that are harmful to the neurons causing neuronal loss and resulting in the pathogenesis of ALS. Several studies analysing differentiated neurons from iPSCs derived from C9-positive HRE carriers have also showed toxic RNA foci and insoluble peptide aggregates generated from repeat-associated non-ATG (RAN) translation may cause gain-of-toxic function of C9ORF72 (20, 24-28).

Because ALS is characterised by late onset of neurodegeneration, we next examined the development of pathogenic responses with and without cell stress stimuli to replicate typical environmental factors that influence the late onset neurodegenerative conditions. Using the cell lines, we also measured the effect of C9ORF72 HRE on endoplasmic reticulum (ER) stress responses and apoptotic cell death in which we observed in the C9-positive cell lines, C9ORF72 isoform a mRNA level is decreased whereas C9ORF72 isoform b mRNA level is strongly increased therefore in C9-positive cell lines, tunicamycin and thapsigargin do not have any further effect on levels of either isoform, suggesting that the C9ORF72 expansion has activated ER stress that cannot further be activated by tunicamycin and thapsigargin, perhaps due to C9ORF72 isoform b upregulation.

Various studies have been performed to investigate the protein expression of C9ORF72 in human tissues (4, 29-31) and cell lines (10, 32). C9ORF72-L and C9ORF72-S have different subcellular localizations in neurons of human tissues as C9ORF72-L is localized throughout the cytoplasm of spinal motor neurons and cerebellar Purkinje cells whereas C9ORF72-S was localized to the nuclear membrane of healthy neurons and was mislocalized to the plasma membrane in diseased spinal motor neurons (33). Using a limited number of samples, they showed that C9ORF72-L protein isoform is only marginally detected in lumbar spinal cord samples from 3 expansion repeat carriers

and 3 SALS cases, whereas levels of C9ORF72-S protein in spinal cord samples in 3 SALS cases were also not significantly changed compared with 3 C9-positive ALS cases (33).

In our study, a single band was observed at approximately 54kDa corresponding in size to the predicted molecular weight of the C9ORF72 long isoform (C9ORF72-L) that indicates C9ORF72-L is the predominantly expressed C9ORF72 protein in human and we did not detect any band corresponding to C9ORF72-S protein that is in agreement with the study by Frick et al.(34)that also did not detect any protein band corresponding to the C9ORF72-S. There was a trend of C9ORF72 protein downregulation in C9-positive cell lines following exposures to tunicamycin and thapsigargin suggesting that C9ORF72 HRE may result in reduced expression of C9ORF72 protein. A previous study has observed the C9ORF72-L and C9ORF72-S protein levels were significantly reduced in the temporal cortex and frontal cortex between 3 SALS cases and 3 C9-positive ALS subjects (33). Furthermore, a study (34) that utilised a greater number of samples has reported that in the cerebellum, C9ORF72-L protein was decreased approximately 20% in patients carrying C9ORF72 HRE compared to controls. This downregulation may be due to the C9ORF72 mutation position in the promoter region of Variant 2(35). This downregulation could also be linked to epigenetic modifications for examples, hypermethylation of CpG islands juxtaposing the repeats or trimethylated histones (35-38).

Rab GTPases have been linked with various neurodegenerative disorders either directly for example, in Charcott-Marie-Tooth type 2B disease (CMT2B) (39) or indirectly as in Alzheimer's disease (AD) (40-43). Rab GTPases alternate between GTP-bound active state and GDP-bound inactive state and are essential in endosomal intracellular trafficking whereas C9ORF72 is colocalized with Rab1, Rab5, Rab7 and Rab11, which are involved in endolysosomal trafficking (10, 32). Further, we aimed to demonstrate a relationship between the presence of C9ORF72 HREs and Rab7 gene expressions. Our finding is that Rab7 is significantly upregulated in LCLs from C9-positive cell lines compared with wild types therefore suggesting that late endosomal activity or autophagy are affected in patients bearing C9ORF72 HRE mutation. Interestingly, we observed that Rab7 and C9ORF72 isoform a mRNA levels are significantly upregulated in wild types upon treatment with tunicamycin and thapsigargin compared to basal level (no treatment) which agrees with the previous findings that C9ORF72 colocalize with Rab proteins such as Rab1, Rab5, Rab7 and Rab11 (44, 45).

A recent study using purified Rab7 GST-fusion protein from E.coli has also reported that Rab7 was able to bind C9ORF72 transfected in Sf9 cells and was further confirmed by size-exclusion chromatography in which Rab7 eluted as a complex with C9ORF72 (46). The upregulation of Rab7 may result in autophagosome accumulation and is also important in mediating autophagic flux increases (47). Autophagosome accumulation may result from either autophagic activation or

dysregulation of intracellular trafficking through the inhibition of downstream steps in autophagy (48, 49). The upregulation of Rab7 in the wild type cell lines indicates that autophagy is enhanced in these cell lines upon ER stress to increase protein aggregates clearance and may also induce apoptosis and neurodegeneration process.

ER stress may trigger theUnfolded Protein Response (UPR) by inducing XBP1 splicing therefore resulting in elevation of HSPA5 and DNAJB9 mRNA levels. We therefore investigated the mRNA levels of HSPA5, XBP1s and DNJAB9 in the lymphoblastoid cell lines in ER stress conditions. HSPA5 mRNA has been reported to be elevated in heat stress condition which is a typical UPR response (50-52), we therefore expected to see an increase of HSPA5 mRNA levels in the lymphoblastoid cell lines. In agreement, we saw a significant increase of HSPA5 mRNA in the wild type lymphoblastoid cell lines upon treatment with tunicamycin or thapsigargin. We observed a modest upregulation upon inducing ER stress with tunicamycin or thapsigargin in the C9 HRE lymphoblastoid cell lines. Interestingly we saw a significant downregulation of HSPA5 mRNA level in C9 HRE compared to wild type lymphoblastoid cell lines upon treatment with tunicamycin. These results suggest that the small increase of HSPA5 mRNA levels in C9 HRE lymphoblastoid cell lines and the significant decrease of HSPA5 mRNA level in C9 HRE compared to wild type cell lines upon tunicamycin treatment might indicate that HSPA5 function is impaired in C9 HRE cell lines therefore affecting the UPR signalling network and causing ER stress leading to the pathogenesis of ALS.

Commented [dBJS2]:

During ER stress, activated IRE1α dimerizes and autophosphorylates and splices a 26-nucleotide intron from XBP1 mRNA resulting in the formation of XBP1s, a transcription factor that upregulates UPR target genes including genes that function in ER-associated degradation (ERAD) and protein folding genes, protein disulphide isomerase (PDI). We investigated the XBP1s mRNA level as it is a direct indication of IRE1 activation and UPR. We therefore expected XBP1s mRNA level to be upregulated in the ER stress condition. In agreement with this, we observed XBP1s mRNA level was upregulated significantly in wild type cells upon treatment with tunicamycin. We also observed the XBP1s mRNA level to be slightly upregulated in wild type cells treated with thapsigargin. However, this upregulation effect was not observed in C9-positive cell lines due to the limited number of C9-positive cell lines. Significant upregulation of XBP1s was again observed in C9-positive cell lines when compared with wild type cell lines upon treatment with tunicamycin. These findings were in agreement with the previous study that shows that in tunicamycin treated cells, XBP1s is important in the transcriptional activation of unfolded protein response element (UPRE) and endoplasmic reticulum stress element (ERSE) of various ER chaperone proteins(51).

We also investigated the mRNA expression of DNAJB9 (ERdj4) in our lymphoblastoid cell lines. DNAJB9 localizes in the endoplasmic reticulum and upon induction by ER stress, it modulates the

ATPase activity of heat shock protein 70 kDa (Hsp70) and suppresses ER stress-induced apoptosis. In wild types, cells treated with tunicamycin or thapsigargin showed upregulations in DNAJB9 mRNA levels but there was no change in the DNAJB9 mRNA expression in C9 HRE cell lines. There is a significant upregulation of DNAJB9 mRNA level in C9-positive cells compared to wild type cells in DMSO or cells treated with thapsigargin. As the activation of DNAJB9 upon ER stress fully requires XBP1 splicing, we could see the similar trends of upregulation in mRNA levels of both XBP1s and DNAJB9 in cells treated with tunicamycin or thapsigargin.

Most of the published studies on apoptosis in ALS were performed in transgenic mutant SOD1 mice (53-56) but limited studies have been carried out in human tissues. In the mutant mouse model, the affected neurons are atrophic and vacuoles containing dilated rough ER, Golgi apparatus and mitochondria are present in the cytoplasm (53). Less than 15% of the spinal cord apoptotic cells show immunoreactivity with neurofilament or glial fibrillary acid protein suggesting that apoptosis causes neuronal and glial cell deaths in the mutant SOD1 mice(55).

We studied the effect of staurosporine on apoptosis in lymphoblastoid cell lines. Staurosporine has been shown to induce apoptosis via intrinsic apoptotic pathways. Staurosporine is a non-selective inhibitor of protein kinase C (PKC) and cyclin-dependent kinase (CDKs) that has been shown to inhibit the proliferation of human epidermoid carcinoma (57) and human leukemic cell line U-937(58). We first performed a dose-response experiment to determine the dose and condition under which staurosporine may induce apoptosis in lymphoblastoid cell lines. From the results, we selected staurosporine concentration of 5 µM and exposure time for 4 hours because the dose-response experiments suggested that this dose and condition produced sufficient cell deaths in lymphoblastoid cell lines. Using the condition of 5 µM staurosporine for 4 hours, we investigated the effect of C9 HRE on the apoptosis events in the lymphoblastoid cell lines.

The cytotoxic effects of staurosporine depend on the cell lines as was demonstrated in the small cell lung carcinoma cells (SCLC). A study has utilized four SCLC cell lines which were SCLC-24H, GLC-2, GLC-36, H1184 and H146 and staurosporine was observed to have varied cytotoxic effect in the different cell lines(59). In their study SCLC-24H cells were almost robust against staurosporine treatment whereas exposures to staurosporine in GLC-2, GLC-36, H1184 and H146 cell lines produced 30% cytotoxicity after 24 hours and to approximately 50% cytotoxicity after 48 hours (59). Another study has also used staurosporine to induce apoptosis in the non-malignant human breast HBL-100 cell line and the T47D malignant breast cell line (60). Treatment with 50 µM staurosporine in these cell lines resulted in shrunken cells and condensed nuclear material that fragmented into electron dense bodies (60).

Our data indicated that the percentage of apoptotic cells was higher in C9-positive cell lines with or without staurosporine treatment when comparing to wild types, therefore suggesting C9 HRE may aggravate cell death in lymphoblastoid cell lines. The upregulation of lymphoblastoid cells apoptosis may be achieved by the activation of pro-apoptotic pathways or inactivation of anti-apoptotic pathways. Earlier studies have demonstrated that in human ALS tissues, Bcl-2 mRNA levels were decreased whereas BAX mRNA level was increased (61, 62). In SOD1 mutant transgenic mice models of ALS (G85R, G37R and G93A), activation of caspase-1 occurs early before neuronal death followed by caspase-3 activation which occurs at or prior to the onset of motor axon loss and the appearance of apoptotic morphology. This sequential caspase activation only occurs in the spinal cord and cortex, regions that are affected by neurodegeneration in ALS (56).

The molecular mechanism through which C9 HRE causes motor neuron death in ALS pathogenesis remains under investigation. Loss of function has been attributed to reduced C9ORF72 expression, haploinsufficiency due to transcriptional instability and epigenetic silencing and histone trimethylation in the blood and cerebellum of C9ORF72-positive ALS and FTD patients. Gain of function is also implicated through the formation and aggregation of toxic RNA foci in C9ORF72-ALS/FTD patients and repeat-associated non-ATG (RAN) translation to produce dipeptide repeat (DPR) proteins which are glycine–alanine (GA), glycine–arginine (GR), proline–alanine (PA), proline–arginine (PR) and glycine–proline (GP). Even though their functions in the pathogenesis of ALS are still under investigation, DPR inclusions have been observed to colocalize with p62 in the cerebellum and frontal cortex of ALS and FTD subjects carrying C9 hexanucleotide repeat expansions (63, 64) but were rarely colocalize with TDP-43 in the spinal cord of C9-positive ALS (65). The accumulations of DPRs in the nucleus resulting in the impaired ribosomal biogenesis, nucleolar stress, nuclear transport defects, modifications in RNA processing and protein mislocalization.

C9ORF72 HRE also results in the formation of R-loops that impair DNA Damage Response (DDR) causing DNA damage. The unrepaired DNA damage leads to increase in apoptosis events in neurons. Furthermore, our findings show that apoptosis was increased in the C9-positive cell lines thus the expression of initiator caspases such as caspase-3 should be investigated using Western blotting to understand the apoptosis mechanism of staurosporine-induced apoptosis in ALS pathogenesis.

DECLARATIONS

Acknowledgements

This work is dedicated to the memory of Jackie de Belleroche, an intelligent woman with passion and dedication who has contributed to scientific progress in the study of ALS. She was a mentor to all of us in her lab and she will always be. We are grateful to the tissue donors and their relatives involved

in this research through the Imperial College ALS Tissue Bank and the Brains for Dementia Research Brain Bank, King's College London. We thank Alex Morris, Midhat Salman and Luigi Montibeller from the Neurogenetics Group for their support.We are grateful to Majlis Amanah Rakyat (MARA) Malaysia for the PhD financial assistance.

Contributions

IB and JB designed research; IB performed research; JB contributed reagents/analytical tools;

IB and JB analysed data; and IB wrote the manuscript. All authors read and approved the final

manuscript.

Ethics declarations

Ethics approval and consent to participate

This study was approved by the Riverside Research Ethics Committee and was carried out according to their guidelines. All clinical diagnoses were confirmed neuropathologically at postmortem.

Consent for publication

Not applicable.

Competing interests

The authors declare that they have no competing interests.

Data availability statement

Anonymized data supporting the findings of this study will be shared by reasonable request from any qualified investigator during three years after the publication of the study. The data are not publicly available due to privacy or ethical restrictions.

REFERENCES

1. Robberecht W, Philips T. The changing scene of amyotrophic lateral sclerosis. Nat Rev Neurosci. 2013;14(4):248-64.

2. Logroscino G, Traynor BJ, Hardiman O, Chiò A, Mitchell D, Swingler RJ, et al. Incidence of amyotrophic lateral sclerosis in Europe. Journal of Neurology, Neurosurgery & Psychiatry. 2010;81(4):385-90.

3. Morita M, Al-Chalabi A, Andersen PM, Hosler B, Sapp P, Englund E, et al. A locus on chromosome 9p confers susceptibility to ALS and frontotemporal dementia. Neurology. 2006;66(6):839-44.

4. DeJesus-Hernandez M, Mackenzie Ian R, Boeve Bradley F, Boxer Adam L, Baker M, Rutherford Nicola J, et al. Expanded GGGGCC Hexanucleotide Repeat in Noncoding Region of C9ORF72 Causes Chromosome 9p-Linked FTD and ALS. Neuron. 2011;72(2):245-56.

5. Renton Alan E, Majounie E, Waite A, Simón-Sánchez J, Rollinson S, Gibbs JR, et al. A Hexanucleotide Repeat Expansion in C9ORF72 Is the Cause of Chromosome 9p21-Linked ALS-FTD. Neuron. 2011;72(2):257-68.

6. van Rheenen W, van Blitterswijk M, Huisman MHB, Vlam L, van Doormaal PTC, Seelen M, et al. Hexanucleotide repeat expansions in C9ORF72 in the spectrum of motor neuron diseases. Neurology. 2012;79(9):878-82.

7. Montuschi A, Iazzolino B, Calvo A, Moglia C, Lopiano L, Restagno G, et al. Cognitive correlates in amyotrophic lateral sclerosis: a population-based study in Italy. Journal of Neurology, Neurosurgery & Psychiatry. 2015;86(2):168.

8. Millecamps S, Boillée S, Le Ber I, Seilhean D, Teyssou E, Giraudeau M, et al. Phenotype difference between ALS patients with expanded repeats in C9ORF72 and patients with mutations in other ALS-related genes. Journal of Medical Genetics. 2012;49(4):258.

9. Zhang D, Iyer LM, He F, Aravind L. Discovery of novel DENN proteins: implications for the evolution of eukaryotic intracellular membrane structures and human disease. Frontiers Genetics. 2012;3(null):283.

10. Levine TP, Daniels RD, Gatta AT, Wong LH, Hayes MJ. The product of C9orf72, a gene strongly implicated in neurodegeneration, is structurally related to DENN Rab-GEFs. Bioinformatics. 2013.

11. Hetz C, Saxena S. ER stress and the unfolded protein response in neurodegeneration. Nature Reviews Neurology. 2017;13(8):477-91.

12. Prell T, Lautenschläger J, Weidemann L, Ruhmer J, Witte OW, Grosskreutz J. Endoplasmic reticulum stress is accompanied by activation of NF-κB in amyotrophic lateral sclerosis. Journal of Neuroimmunology. 2014;270(1–2):29-36.

13. Oakes S, Papa F. The Role of Endoplasmic Reticulum Stress in Human Pathology. Annual Review of Pathology: Mechanisms of Disease. 2015;10(1):173-94.

14. Urra H, Dufey E, Lisbona F, Rojas-Rivera D, Hetz C. When ER stress reaches a dead end. Biochimica et Biophysica Acta (BBA) - Molecular Cell Research. 2013;1833:3507-17.

15. Honig LS, Rosenberg RN. Apoptosis and neurologic disease. The American Journal of Medicine. 2000;108(4):317-30.

16. Troost D, Aten J, Morsink F, de Jong JMBV. Apoptosis in amyotrophic lateral sclerosis is not restricted to motor neurons. Bcl-2 expression is increased in unaffected post-central gyrus. Neuropathology and Applied Neurobiology. 1995;21(6):498-504.

17. Rabizadeh S, Gralla EB, Borchelt DR, Gwinn R, Valentine JS, Sisodia S, et al. Mutations associated with amyotrophic lateral sclerosis convert superoxide dismutase from an antiapoptotic gene to a proapoptotic gene: studies in yeast and neural cells. Proceedings of the National Academy of Sciences. 1995;92(7):3024-8.

18. Durham HD, Roy J, Dong L, Figlewic DA. Aggregation of Mutant Cu/Zn Superoxide Dismutase Proteins in a Culture Model of ALS. Journal of Neuropathology & Experimental Neurology. 1997;56(5):523-30.

19. Ciura S, Lattante S, Le Ber I, Latouche M, Tostivint H, Brice A, et al. Loss of function of C9orf72 causes motor deficits in a zebrafish model of amyotrophic lateral sclerosis. Annals of Neurology. 2013;74(2):180-7.

20. Donnelly Christopher J, Zhang P-W, Pham Jacqueline T, Haeusler Aaron R, Mistry Nipun A, Vidensky S, et al. RNA Toxicity from the ALS/FTD C9ORF72 Expansion Is Mitigated by Antisense Intervention. Neuron. 2013;80(2):415-28.

21. Banerjee A, Lang J-Y, Hung M-C, Sengupta K, Banerjee SK, Baksi K, et al. Unfolded Protein Response Is Required in nu/nu Mice Microvasculature for Treating Breast Tumor with Tunicamycin. Journal of Biological Chemistry 2011;286 29127-38.

22. Oslowski CM, Urano F. Measuring ER stress and the unfolded protein response using mammalian tissue culture system. Methods in enzymology. 2011;490:71-92.

23. Cherfils J, Zeghouf M. Regulation of Small GTPases by GEFs, GAPs, and GDIs. Physiological Reviews. 2013;93(1):269-309.

24. Almeida S, Gascon E, Tran H, Chou HJ, Gendron TF, DeGroot S, et al. Modeling key pathological features of frontotemporal dementia with C9ORF72 repeat expansion in iPSC-derived human neurons. Acta Neuropathologica. 2013;126:385-99.

25. Ash Peter EA, Bieniek Kevin F, Gendron Tania F, Caulfield T, Lin W-L, DeJesus-Hernandez M, et al. Unconventional Translation of C9ORF72 GGGGCC Expansion Generates Insoluble Polypeptides Specific to c9FTD/ALS. Neuron. 2013;77:639-46.

26. Lagier-Tourenne C, Baughn M, Rigo F, Sun S, Liu P, Li H-R, et al. Targeted degradation of sense and antisense C9orf72 RNA foci as therapy for ALS and frontotemporal degeneration. Proceedings of the National Academy of Sciences. 2013;110(47):E4530-E9.

27. Mori K, Weng S-M, Arzberger T, May S, Rentzsch K, Kremmer E, et al. The C9orf72 GGGGCC Repeat Is Translated into Aggregating Dipeptide-Repeat Proteins in FTLD/ALS. Science. 2013;339(6125):1335-8.

28. Sareen D, O'Rourke JG, Meera P, Muhammad AKMG, Grant S, Simpkinson M, et al. Targeting RNA Foci in iPSC-Derived Motor Neurons from ALS Patients with a C9ORF72 Repeat Expansion. Science Translational Medicine. 2013;5(208):208ra149.

29. Cooper-Knock J, Hewitt C, Highley JR, Brockington A, Milano A, Man S, et al. Clinico-pathological features in amyotrophic lateral sclerosis with expansions in C9ORF72. Brain. 2012;135(3):751-64.

30. Gijselinck I, Van Langenhove T, van der Zee J, Sleegers K, Philtjens S, Kleinberger G, et al. A C9orf72 promoter repeat expansion in a Flanders-Belgian cohort with disorders of the frontotemporal lobar degeneration-amyotrophic lateral sclerosis spectrum: a gene identification study. The Lancet Neurology. 2012;11(1):54-65.

31. Hsiung G-YR, DeJesus-Hernandez M, Feldman HH, Sengdy P, Bouchard-Kerr P, Dwosh E, et al. Clinical and pathological features of familial frontotemporal dementia caused by C9ORF72 mutation on chromosome 9p. Brain. 2012;135(3):709-22.

32. Farg MA, Sundaramoorthy V, Sultana JM, Yang S, Atkinson RAK, Levina V, et al. C9ORF72, implicated in amytrophic lateral sclerosis and frontotemporal dementia, regulates endosomal trafficking. Human Molecular Genetics. 2014;23:3579-95.

33. Xiao S, Macnair L, McGoldrick P, McKeever PM, Robertson J. Isoform-specific antibodies reveal distinct subcellular localizations of C9orf72 in amyotrophic lateral sclerosis. Ann Neurol. 2015;78(4):568.

34. Frick P, Sellier C, Mackenzie IRA, Cheng C-Y, Tahraoui-Bories J, Martinat C, et al. Novel antibodies reveal presynaptic localization of C9orf72 protein and reduced protein levels in C9orf72 mutation carriers. Acta Neuropathologica Communications. 2018;6:72.

35. Xi Z, Zhang M, Bruni AC, Maletta RG, Colao R, Fratta P, et al. The C9orf72 repeat expansion itself is methylated in ALS and FTLD patients. Acta Neuropathologica. 2015;129:715-27.

36. Belzil VV, Bauer PO, Prudencio M, Gendron TF, Stetler CT, Yan IK, et al. Reduced C9orf72 gene expression in c9FTD/ALS is caused by histone trimethylation, an epigenetic event detectable in blood. Acta Neuropathologica. 2013;126(6):895-905.

37. Xi Z, Zinman L, Grinberg Y, et al. Investigation of c9orf72 in 4 neurodegenerative disorders. Archives of Neurology. 2012;69(12):1583-90.

38. Liu EY, Russ J, Wu K, Neal D, Suh E, McNally AG, et al. C9orf72 hypermethylation protects against repeat expansion-associated pathology in ALS/FTD. Acta Neuropathologica. 2014;128(4):525-41.

39. Meggouh F, Bienfait HME, Weterman MAJ, de Visser M, Baas F. Charcot-Marie-Tooth disease due to a de novo mutation of the RAB7 gene. Neurology. 2006;67:1476 LP - 8.

40. Ba L, Chen X-H, Chen Y-L, Nie Q, Li Z-J, Ding F-F, et al. Distinct Rab7-related Endosomal–Autophagic–Lysosomal Dysregulation Observed in Cortex and Hippocampus in APPswe/PSEN1dE9 Mouse Model of Alzheimer's Disease. Chinese Medical Journal. 2017;130(24):2941-50.

41. Ginsberg SD, Alldred MJ, Counts SE, Cataldo AM, Neve RL, Jiang Y, et al. Microarray analysis of hippocampal CA1 neurons implicates early endosomal dysfunction during Alzheimer's disease progression. Biological psychiatry. 2010;68:885-93.

42. Zhang X, Huang TY, Yancey J, Luo H, Zhang Y-w. Role of Rab GTPases in Alzheimer's Disease. ACS Chemical Neuroscience. 2019;10:828-38.

43. Xu W, Fang F, Ding J, Wu C. Dysregulation of Rab5-mediated endocytic pathways in Alzheimer's disease. Traffic. 2018;19(4):253-62.

44. Tang BL. C9orf72's Interaction with Rab GTPases-Modulation of Membrane Traffic and Autophagy. Frontiers in cellular neuroscience. 2016;10:228.

45. Farg MA, Sundaramoorthy V, Sultana JM, Yang S, Atkinson RAK, Levina V, et al. C9ORF72, implicated in amytrophic lateral sclerosis and frontotemporal dementia, regulates endosomal trafficking. Human Molecular Genetics. 2014;23(13):3579-95.

46. Iyer S, Subramanian V, Acharya KR. C9orf72, a protein associated with amyotrophic lateral sclerosis (ALS) is a guanine nucleotide exchange factor. PeerJ. 2018;6:e5815-e.

47. Hariharan N, Maejima Y, Nakae J, Paik J, DePinho Ronald A, Sadoshima J. Deacetylation of FoxO by Sirt1 Plays an Essential Role in Mediating Starvation-Induced Autophagy in Cardiac Myocytes. Circulation Research. 2010;107:1470-82.

48. Wong E, Cuervo AM. Autophagy gone awry in neurodegenerative diseases. Nature Neuroscience. 2010;13:805.

49. Levine B, Kroemer G. Autophagy in the Pathogenesis of Disease. Cell. 2008;132(1):27-42.

50. Gessner DK, Schlegel G, Ringseis R, Schwarz FJ, Eder K. Up-regulation of endoplasmic reticulum stress induced genes of the unfolded protein response in the liver of periparturient dairy cows. BMC Veterinary Research. 2014;10:46.

51. Heldens L, Hensen SMM, Onnekink C, van Genesen ST, Dirks RP, Lubsen NH. An Atypical Unfolded Protein Response in Heat Shocked Cells. PLOS ONE. 2011;6:e23512.

52. Enogieru AB, Omoruyi SI, Hiss DC, Ekpo OE. GRP78/BIP/HSPA5 as a Therapeutic Target in Models of Parkinson Disease: A Mini Review. Advances in Pharmacological Sciences. 2019;2019:11.

53. Dal Canto MC, Gurney ME. Neuropathological changes in two lines of mice carrying a transgene for mutant human Cu,Zn SOD, and in mice overexpressing wild type human SOD: a model of familial amyotrophic lateral sclerosis (FALS). Brain Research. 1995;676(1):25-40.

54. Migheli A, Atzori C, Piva R, Tortarolo M, Girelli M, Schiffer D, et al. Lack of apoptosis in mice with ALS. Nature Medicine. 1999;5:966-7.

55. Vukosavic S, Stefanis L, Jackson-Lewis V, Guégan C, Romero N, Chen C, et al. Delaying Caspase Activation by Bcl-2: A Clue to Disease Retardation in a Transgenic Mouse Model of Amyotrophic Lateral Sclerosis. The Journal of Neuroscience. 2000;20(24):9119-25.

56. Pasinelli P, Borchelt DR, Houseweart MK, Cleveland DW, Brown RH. Caspase-1 is activated in neural cells and tissue with amyotrophic lateral sclerosis-associated mutations in copper-zinc superoxide dismutase. Proceedings of the National Academy of Sciences. 1998;95(26):15763-8.

57. Akinaga S, Nomura K, Gomi K, Okabe M. No TitleEffect of UCN- 01, a selective inhibitor of protein kinase C, on the cell-cycle distribution of human epidermoid carcinoma, A431 cells. Cancer Chemother Pharmacol. 1994;33:273-80.

58. Antonsson A, Persson JL. Induction of Apoptosis by Staurosporine Involves the Inhibition of Expression of the Major Cell Cycle Proteins at the G2/M Checkpoint Accompanied by Alterations in Erk and Akt Kinase Activities. Anticancer Research. 2009;29(8):2893-8.

59. Murmann T, Carrillo-García C, Veit N, Courts C, Glassmann A, Janzen V, et al. Staurosporine and Extracellular Matrix Proteins Mediate the Conversion of Small Cell Lung Carcinoma Cells into a Neuron-Like Phenotype. PLOS ONE. 2014;9:e86910.

60. McKeague AL, Wilson DJ, Nelson J. Staurosporine-induced apoptosis and hydrogen peroxide-induced necrosis in two human breast cell lines. British Journal of Cancer. 2003;88:125-31.

61. Mu X, He J, Anderson DW, Springer JE, Trojanowski JQ. Altered expression of bcl-2 and bax mRNA in amyotrophic lateral sclerosis spinal cord motor neurons. Annals of Neurology. 1996;40(3):379-86.

62. Tews D, Goebel H, Meinck H. DNA-fragmentation and apoptosis related proteins of muscle cells in motor neuron disorders. Acta Neurol Scand. 1997;96:380-6.

63. Mackenzie IR, Arzberger T, Kremmer E, Troost D, Lorenzl S, Mori K, et al. Dipeptide repeat protein pathology in C9ORF72 mutation cases: clinico-pathological correlations. Acta Neuropathologica. 2013;126(6):859-79.

64. Mann DMA, Rollinson S, Robinson A, Bennion Callister J, Thompson JC, Snowden JS, et al. Dipeptide repeat proteins are present in the p62 positive inclusions in patients with frontotemporal

lobar degeneration and motor neurone disease associated with expansions in C9ORF72. Acta Neuropathologica Communications. 2013;1:68.

65. Gomez-Deza J, Lee Y-b, Troakes C, Nolan M, Al-Sarraj S, Gallo J-M, et al. Dipeptide repeat protein inclusions are rare in the spinal cord and almost absent from motor neurons in C9ORF72 mutant amyotrophic lateral sclerosis and are unlikely to cause their degeneration. Acta Neuropathologica Communications. 2015;3:38.

SUPPLEMENTARY MATERIALS

Gene	Primer Sequence (5'-3')	qPCR Product Size (bp)
KANK1	GCACCCTGTCGTCTATCAACTC	214
	CTGCTGATTGGCTTTCCTTCT	
KIF21A	GCAGAAGGGCAAGAGATTGGA	183
	TGCTTTCTCATATGCCTTTCTCCT	
GAPDH	Proprietary primer set (Primer Design, UK)	118
XBP1s	AGAGTCTGATATCCTGTTGG	189
	AGTTCATTAATGGCTTCCAG	
DNAJB9	TTTCCAGACACGCCAGGATG	195
	GTCCTGCAGTGCTTGCTAGA	
HSPA5	TCAAGTTCTTGGCCGTTCAAGG	145
	AAATAAGCCTAGCGGTTTCTCT	

Table S1: Primers pairs used for quantitative PCR (qPCR).

Staurosporine	Percentage of cell death (%)							
	3 µM				5 µM			
Duration(s) (h, hour)	Total Apoptosis		Necrosis		Total Apoptosis		Necrosis	
	WT	C9	WT	C9	WT	C9	WT	C9
0h	24.13	26.77	0.72	0.74	22.92	17.77	2.39	3.70
2h	21.12	26.32	2.73	1.40	21.83	18.98	5.56	8.56
4h	22.48	25.11	1.62	3.09	22.03	25.14	5.19	5.11
24h	55.78	57.32	14.98	13.72	19.34	27.83	30.61	23.47

Table S2: The rates of total apoptosis and necrosis in wild type (WT) and C9ORF72-positive (C9) cell lines upon treatment with 5 and 3 µM staurosporine for 0, 2, 4 and 24 hour(s).

Group	**Wild types (n =12)**		**C9-positive (n =12)**	
Treatment	**Media**	**+ ST**	**Media**	**+ ST**
TOTAL APOPTOSIS				
Mean ± S.E.M (%)	21.06 ± 1.843	24.96 ± 1.890	23.71 ± 2.742	32.24 ± 3.542
p-value				
	0.0474(*)		0.0028(**)	
WT vs C9	0.4312(ns)			
WT+ST vs C9+ST	0.0833(ns)			
NECROSIS				
Mean ± S.E.M (%)	1.647 ±0.353	4.298 ± 0.851	3.636 ± 0.869	6.105 ± 1.304
p-value				
	0.0046(**)		0.0378(*)	
WT vs C9	0.0454(*)			
WT+ST vs C9+ST	0.2582(ns)			

Table S3: The rates of total apoptosis and necrosis in wild types (WT) and C9ORF72-positive (C9) cell lines upon treatment with 5 µM staurosporine (ST) for 4 hours.